

# Bias of integrated optics Pockels cell high-voltage sensors

Nicolas A.F. Jaeger and Farnoosh Rahmatian

University of British Columbia, Department of Electrical Engineering  
Vancouver, BC, Canada V6T 1Z4

## ABSTRACT

The results of measurements of the intrinsic phase-differences of titanium-indiffused lithium niobate waveguides, for use in integrated optics Pockels cell high-voltage sensors, are presented. The dependencies of the intrinsic phase-differences of these waveguides on their lengths and widths are investigated; a change of between  $4.9$  and  $5.9^\circ/\mu\text{m}/\text{mm}$  was obtained. Also, the change in the intrinsic phase-difference as a function of both temperature and time was investigated; a typical change of  $0.02^\circ/\text{C}/\text{mm}$  was measured and, following a small initial change, the bias was found not to drift with time. Some suggestions for possible post-processing of the output signals, of the integrated optics Pockels cell high-voltage sensors, to increase the dynamic range and to compensate for small changes in the bias, are presented.

## 1. INTRODUCTION

Optical sensors have found various applications in industrial environments<sup>1</sup>. Several optical devices have been suggested and developed, over the last few years, for the measurement of voltage, current, or other parameters in high-voltage environments<sup>2-7</sup>. In particular, systems using fibre optics offer immunity to electromagnetic interference. This immunity may be important when a sensor is employed in the high-voltage environment, where very large transient fields can occur. Integrated optics Pockels cells (IOPCs), to be used as electric field sensors in high-voltage environments, have been previously introduced<sup>8,9</sup>. Here, several issues related to the bias of these sensors are discussed; also, for completeness, a brief description of these devices is provided first.

## 2. DEVICE DESCRIPTION

Basically, an IOPC consists of a sensor-head, to be placed in the high-voltage environment, optical fibres to transmit light to and from the sensor-head, a laser diode as a light source, and an optoelectronic conversion unit to measure the optical signals. The sensor-head consists of a waveguide fabricated by diffusing a strip of titanium into a y-cut substrate of lithium niobate, the waveguide being parallel to the z crystallographic axis. The dimensions of the pre-diffusion titanium strip are chosen so that the waveguide formed, after the diffusion, supports only two modes: the fundamental TE-like mode and the fundamental TM-like mode. Polarized light, from the laser diode, is transmitted to the sensor-head using an input fibre which is polarization maintaining (PM). The input fibre is aligned with the end of the waveguide in the sensor-head such that the PM axis of the fibre is at about  $45^\circ$  to the x and y crystallographic axes of the lithium niobate substrate. This alignment is intended to result in nearly equal amounts of optical

power in the fundamental TE- and TM-like modes, supported by the waveguide, at the output of the waveguide. The propagation constants of the two modes are slightly different; therefore, when no electric field is applied, the two modes have an intrinsic phase-difference at the output of the waveguide. Application of an electric field parallel to the y crystallographic axis creates a change in the difference between the phase velocities of the two modes of the waveguide. The polarization state at the output of the waveguide will be elliptical with the major and minor axes of the polarization ellipse at about 45° to the x and y crystallographic axis. The output of the waveguide is interrogated using a birefringent PM optical fibre. The fibre is aligned with its PM axes parallel to the principal axes of the polarization ellipse to interrogate the optical powers parallel to these two axes. The two optical powers can be separated and measured individually. The response is normalized by dividing one optical power component by the sum of the two, i.e., the total optical power detected. This normalization is done to make the sensor less susceptible to variations in the total optical power due to vibration or other factors. The applied-electric-field-in/normalized-optical-intensity-out transfer function of the sensor is

$$S = \frac{1 \pm \alpha \cos [(\pi E_y / E_\pi) + \phi_i]}{2} \quad (1)$$

where  $S$  is the normalized output intensity, plus or minus depends on the choice of the output component for the numerator when normalizing, the constant  $\alpha$  is close to, but smaller than, one (typically  $\geq 0.99$ ),  $E_y$  is the electric field parallel to the y crystallographic axis inside the sensor-head,  $E_\pi$  is the half-wave electric field, and  $\phi_i$  is the intrinsic phase-difference (bias) between the two modes supported by the waveguide. Theoretically, the half-wave electric field can be written as

$$E_\pi = \frac{\lambda_o}{2 n_o^3 r_{22} L} \quad (2)$$

where  $\lambda_o$  is the free-space optical wavelength,  $n_o$  is the ordinary refractive index for lithium niobate,  $r_{22}$  is the relevant electro-optic coefficient, and  $L$  is the length of the waveguide.

### 3. DISCUSSION OF FACTORS AFFECTING THE BIAS

For the IOPC to be used as an electric field sensor, a nearly linear transfer function for the sensor is desirable. The transfer function (1) is nearly linear when  $\phi_i = \pi/2$  (90°) and  $(\pi E_y / E_\pi)$  is sufficiently small. For  $\phi_i = \pi/2$  and small  $(\pi E_y / E_\pi)$ , the a.c. component of  $S$ ,  $s$ , can be written as

$$s \approx \mp \frac{\alpha \pi}{2 E_\pi} E_y \quad (3)$$

Lithium niobate based integrated optics modulators used for communication applications are

often biased using a separate pair of electrodes<sup>10</sup>. In such devices, the bias can be controlled by applying an appropriate d.c. voltage to the bias electrodes. As mentioned earlier, the sensor-head of an IOPC is basically a dielectric crystal (lithium niobate) and, preferably, has no metal electrodes, in order to minimize the danger of corona discharge (flash over) when placed in large electric fields. As a result, it is quite inappropriate to use bias electrodes for controlling the intrinsic phase-difference of the sensor-head. Fortunately, the bias of the sensor-head of an IOPC can be set by controlling its fabrication parameters. The results of measurements of the dependence of the intrinsic phase-difference of the sensor on the waveguide's length, waveguide's width, and change in temperature are given in the following sections. The bias drift and some simple post-processing methods to compensate for a non-ideal bias are also presented.

### 3.1. The effect of a waveguide's length on its bias

The intrinsic phase-difference of the IOPC is, theoretically, dependent on the length of the waveguide in the sensor-head,  $L$ , and the difference in the propagation constants of the two modes supported by the waveguide. It can be written as

$$\phi_i = (\beta_{TE} - \beta_{TM}) \times L \quad (4)$$

where  $\beta_{TE}$  and  $\beta_{TM}$  are the propagation constants for the fundamental TE- and TM-like modes, respectively. In order to fabricate properly biased waveguides, a long waveguide can be fabricated first, and its intrinsic phase-difference can be measured. Then, it can be cut to a length for which the intrinsic phase-difference is expected to be close to  $\pi/2$ .

Experiments were conducted to examine the relation between the intrinsic phase-difference and the length of the waveguides; the results are plotted in fig. 1. The waveguides used in this plot are divided into three clusters; each cluster contains waveguides having either 3.0, 3.5, or 4.0  $\mu\text{m}$  pre-diffusion titanium strip widths. This distinction is made in order to be able to discriminate between the effect of the length and the effect of the width of a waveguide on its intrinsic phase-difference. The straight lines in fig. 1 are least-squares-fits to the data points in each cluster. It should be noted that the waveguides used in this plot were not all fabricated at the same time or under identical conditions. The pre-diffusion titanium strip thickness, diffusion time, and diffusion temperature are some factors that may affect  $\beta_{TE}$  and  $\beta_{TM}$  and may, in turn, affect the bias; small variations in the intrinsic phase-differences of the waveguides of similar lengths are observed in fig. 1. The results presented in fig. 1 indicate that (4) holds reasonably well for these waveguides, and can be exploited in fabricating well-biased devices. Fig. 1 shows that a well-biased waveguide should be between 6 and 9 mm long, depending on its other fabrication parameters.

For nearly linear operation, see (1) and (3),  $\phi_i$  can be any odd multiple of  $\pi/2$ . However, it should be noted that the piezoelectric resonance frequencies of the lithium niobate substrates are inversely proportional to the substrate dimensions<sup>9,12</sup>; therefore, to obtain devices having large useable bandwidths, their sensor-heads should be small. This is a reason for trying to obtain waveguides with  $\phi_i = \pi/2$ , and not just any odd multiple of  $\pi/2$ .

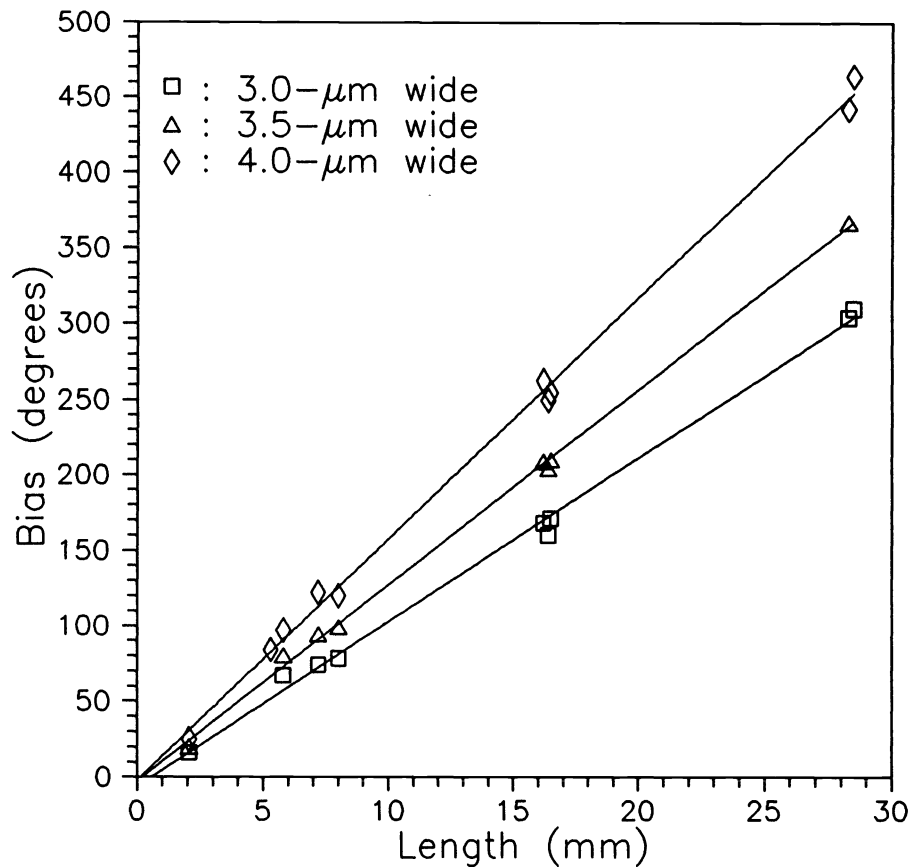


Fig. 1. The intrinsic phase-difference (bias) as a function of the length.

### 3.2. The effect of a waveguide's width on its bias

A waveguide's width also affects its intrinsic phase-difference. Using simple models, based on channel waveguides having rectangular cross-sections, one can show that wider waveguides have larger intrinsic phase-differences<sup>12</sup>. Experiments were conducted to investigate the effect of a waveguide's width on its bias. Fig. 2 shows a plot of the measured intrinsic phase-differences for several waveguides as functions of their pre-diffusion titanium strip widths. Again, in order to be able to differentiate between the effect of the width and the effect of the length of a waveguide on its bias, the data presented in fig. 2 are arranged in three clusters according to the waveguide length: these waveguides were 8, 16, or 28 mm long. As predicted, the wider the waveguide the larger the intrinsic phase-difference. It should be noted that each data point in fig. 2 is an average intrinsic phase-difference for several waveguides having the same length and the same pre-diffusion titanium strip width, but possibly differing in their other fabrication parameters; the symbol height represents the difference between the maximum and minimum measured values. From fig. 2, the change in the intrinsic phase-difference per unit width per unit length of a waveguide is between 4.9 and 5.9°/μm/mm. These results, together

with the results presented in fig. 1, can be used in designing well-biased waveguides. For example, several waveguides with pre-diffusion titanium strips 3 to 4  $\mu\text{m}$  wide, varying by 0.1  $\mu\text{m}$ , can be made in a single substrate. Then, the waveguides can be cut to about 7 mm. It can be deduced from fig.'s 1 and 2 that one of these waveguides should have an intrinsic phase-difference which is within a few degrees of  $90^\circ$ . Hence, the intrinsic phase-differences of all of these waveguides can be measured, and the one with the intrinsic phase-difference closest to  $90^\circ$  can be chosen to be used for the sensor.

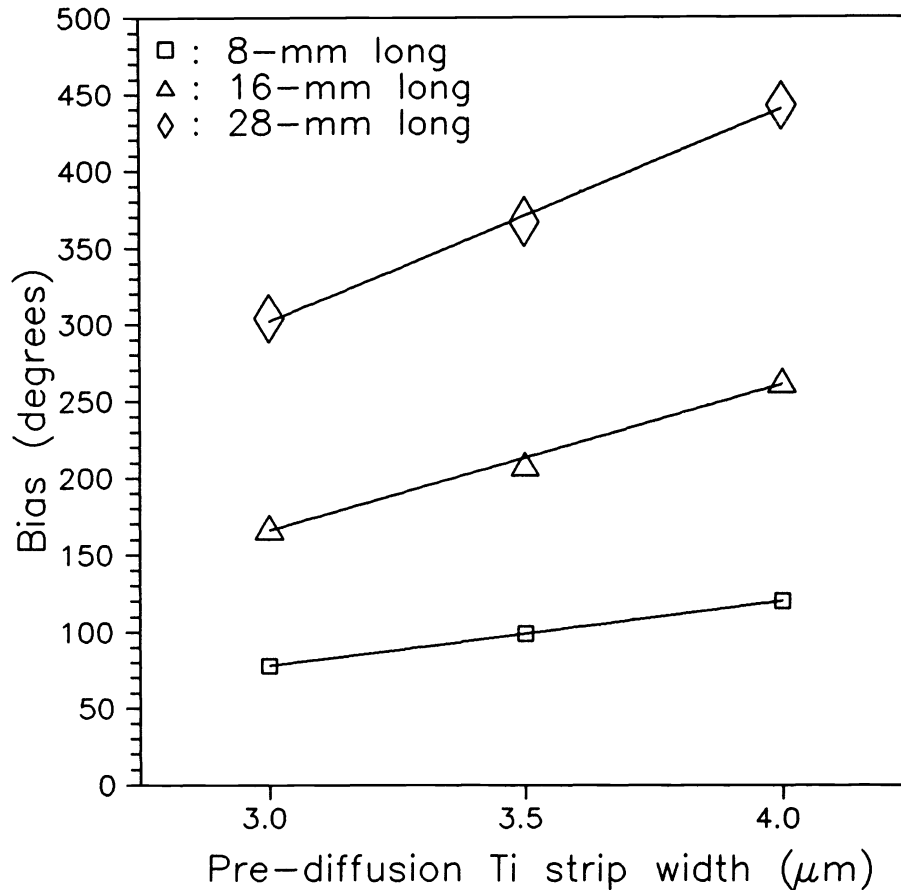


Fig. 2. The intrinsic phase-difference (bias) as a function of the pre-diffusion titanium strip width.

As mentioned before, the wider the waveguides are the larger their intrinsic phase-differences will be. It is, therefore, appropriate to make a waveguide as wide as possible to be able to minimize the length of a well-biased waveguide. It should be noted, however, that there is a limit to how wide a waveguide can be; if the waveguide is too wide, it will support more modes than just the two fundamental ones. In the experiments conducted, waveguides having pre-diffusion titanium strip widths  $\geq 4.5 \mu\text{m}$  generally supported more modes than the two

fundamental ones when  $\lambda_0 = 670$  nm; thus, they were not used in the sensors.

### 3.3. The effects of temperature on the bias

A change in temperature can also affect the intrinsic phase-difference of a waveguide. Therefore, experiments were conducted to observe the dependence of a waveguide's bias on temperature. Several samples, containing waveguides, were placed on a heating stage, and the intrinsic phase-differences of the waveguides were measured as the stage temperature was increased from room temperature,  $\sim 20^\circ\text{C}$ , to  $\sim 70^\circ\text{C}$ . For each reading, once the temperature of the stage was determined,  $\sim 10$  minutes were allowed to elapse before the measurement was taken and recorded, so that the sample could reach the nominal stage temperature. The results for nine waveguides are plotted in fig. 3. The straight lines are least-squares-fits to the data points for individual waveguides. All of these waveguides were 28 mm long. The pre-diffusion titanium strip widths were 3.0, 3.5, and 4.0  $\mu\text{m}$  for the waveguides represented by the bottom three, the middle three, and the top three best-fit lines, respectively. Fig. 3 shows that a typical change in the bias per degree change in temperature per unit length of a waveguide is  $\sim 0.02^\circ\text{C}/\text{mm}$ .

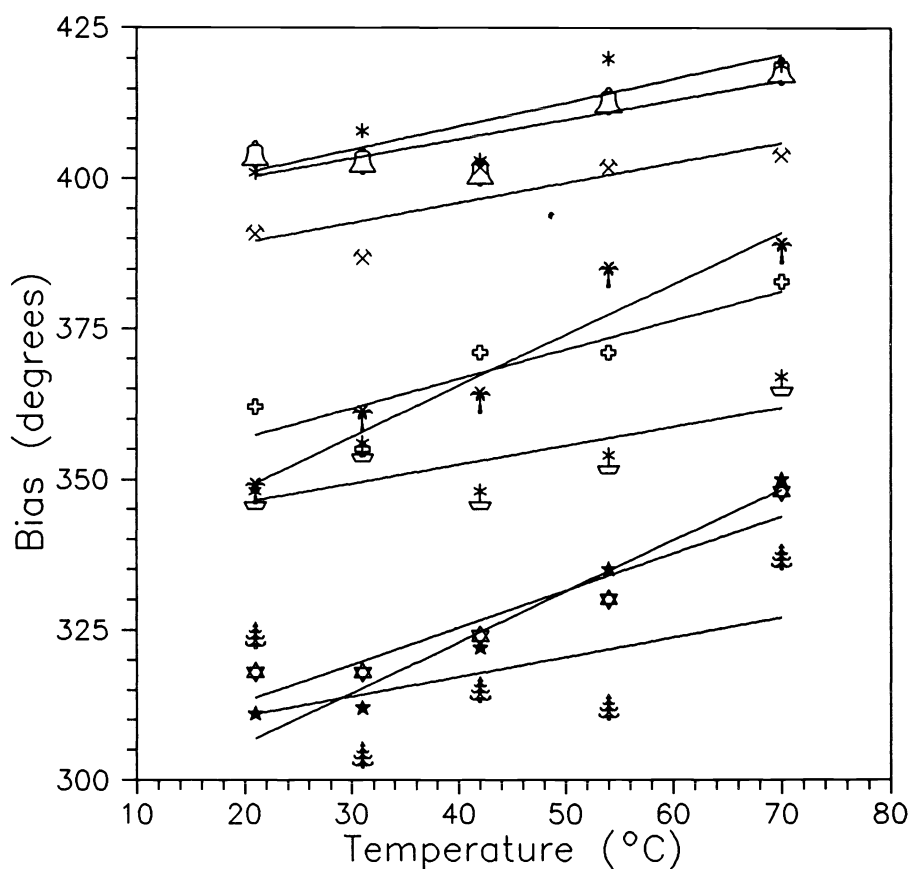


Fig. 3. The intrinsic phase-difference (bias) as a function of temperature.

### 3.4. Stability

The change in a waveguide's intrinsic phase-difference with time can affect the accuracy of the measurements made using the device. The bias drift is mainly attributed to the optical damage in the waveguide. The optical damage for x- and y-propagating waveguides in lithium niobate are reported to be significant for optical powers in excess of a few  $\mu\text{W}$  when operating with visible light<sup>13</sup>. For z-propagating waveguides, however, the optical damage is expected to be very small as compared to those for x- or y- propagating waveguides<sup>11</sup>. Fig.'s 4a and 4b show the transfer functions for one waveguide after the laser was on for one minute and for two hours, respectively; the output optical power was  $\sim 200 \mu\text{W}$ . A bias drift of about  $2^\circ$  after 2 hours was measured. No further noticeable bias drift was observed as the laser was left on for several hours ( $> 20$  hours). In the applications for which these sensors are intended, e.g., metering high-voltage a.c. signals, the sensor is rarely (if ever) off. Therefore, this initial bias drift should not affect the performance as long as the stabilized bias is close to its intended value of  $90^\circ$ . Even though this drift is very small, practically negligible, it can be further reduced by making systems which operate at longer wavelengths, e.g.,  $1.3 \mu\text{m}$ . It is reported<sup>13</sup> that optical damage is negligible for optical powers less than  $20 \text{ mW}$  when operating at  $\lambda_o = 1.3 \mu\text{m}$ .

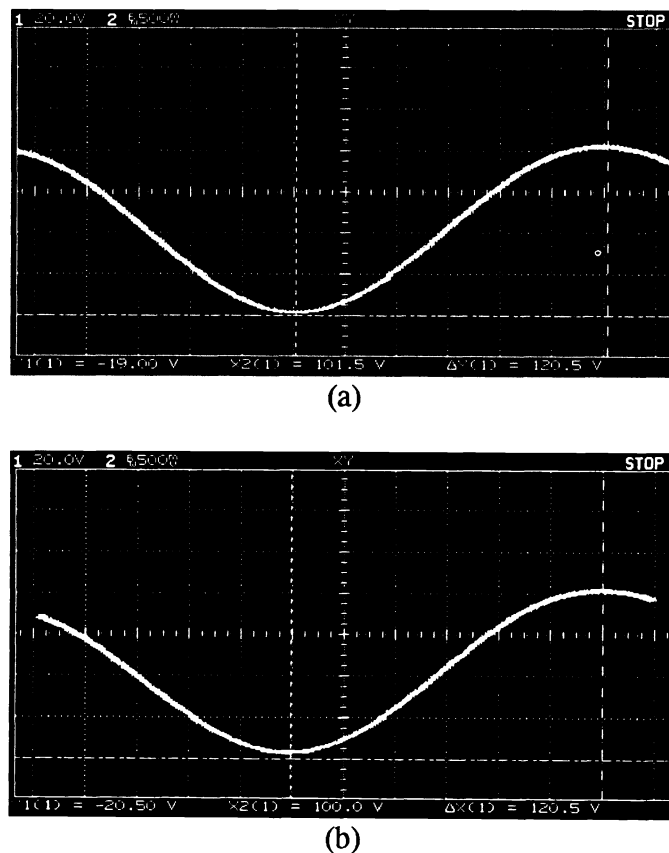


Fig. 4. The transfer function of an IOPC (a) one minute and (b) two hours after turning the laser on.

### 3.5. Post-processing

The dynamic range of the IOPC, i.e., the range within which the sensor can be used, is restricted to  $\pm 8^\circ$  of a bias point of  $90^\circ$ , for the error introduced by (3) to be less than 0.3%<sup>14</sup>. For better signal-to-noise ratios, increasing the dynamic range of the sensor is desirable. The dynamic range can be increased by using approximations other than  $\sin(x) \approx x$ , which was used to obtain (3) from (1). For instance<sup>12</sup>, the approximation  $[\sin(x) + k \sin^3(x)] \approx x$  will introduce less than 0.1% error for a dynamic range of  $\pm 30^\circ$  about a bias point of  $90^\circ$ , if the constant  $k$  is chosen properly ( $k = 0.188$ ). For implementing this technique, when metering a 60 Hz signal for example, the output of the sensor can be a.c. coupled to eliminate the d.c. value in (1). Then, a digital processing unit can be designed to sample the output and to carry out the tasks of additions and multiplications in real-time to perform the calculations suggested above.

A digital sampling unit, together with a micro-computer, can also be used for post-processing the output. This post-processing can be used to compensate for bias changes and to increase the dynamic range of the sensor. For example, the sampling unit can sample the output of the IOPC and transfer the results to the computer. The parameters of the transfer function (1) can be measured, at the time of fabrication, and stored in the computer. Since both components of the output of the sensor-head are measured, the intrinsic phase-difference,  $\phi_i$ , can be continuously updated. The computer can use the transfer function and the values obtained by the sampling unit to calculate  $E_y$ . In this way, the dynamic range is increased to close to  $\pi$ .

## 4. SUMMARY

The effects of a waveguide's length and width on its intrinsic phase-difference have been investigated. Longer and wider waveguides have larger intrinsic phase-difference as compared to shorter and narrower ones. Well-biased waveguides 6 to 9 mm long have been successfully fabricated. The effect of temperature changes on the bias of the waveguides has also been examined; for the waveguides studied, a typical change in bias of  $0.02^\circ/\text{C}/\text{mm}$  was measured. Following a small initial change, the bias appeared to be stable with time. Post-processing can increase the dynamic range of the sensor and/or compensate for any of the observed bias changes.

## 5. ACKNOWLEDGEMENT

The authors wish to thank the Science Council of British Columbia and the Natural Sciences and Engineering Research Council of Canada for their financial support of this work.

## 6. REFERENCES

1. J. Dakin and B. Culshaw, Optical Fiber Sensors: Principles and Components, Artech House, Norwood, 1988.
2. S. Kobayashi, A. Horide, I. Takagi, M. Higaki, G. Takahashi, E. Mori, and T. Yamagiwa, "Development and field test evaluation of optical current and voltage transformers for gas insulated switchgear," *IEEE Trans. on Power Delivery*, vol. 7, no. 2, pp. 815-821, 1992.

3. J. Beatty, T. Meyer, and E.A. Ulmer, "Application and Field Trial of High Accuracy Optical Current Transducer for Electrical Power Systems," presented at the *Conference on Optical Sensing in Utility Applications*, San Francisco, CA, May 1991.
4. R.F. Cook, "Optical sensing-metering systems," presented at the *EEI-AEIC meter & service committee conference*, pp. 1-4, Washington, D.C., April 3, 1990.
5. T.D. Maffetone and T.M. McClelland, "345 kV substation optical current measurement system for revenue metering and protective relaying," presented at the *IEEE/PES Winter Meeting*, pp. 1-8, New York, NY, 1991.
6. T. Mitsui, K. Hosoe, H. Usami, and S. Miyamoto, "Development of fibre-optic voltage sensors and magnetic-field sensors," *IEEE Trans. on Power Delivery*, vol. PWRD-2, no. 1, pp. 87-93, Jan. 1987.
7. T. Sawa, K. Kurosawa, T. Kaminishi, and T. Yokata, "Development of Optical Instrument Transformers," *IEEE Trans. on Power Delivery*, vol. 5, no. 2, pp. 884-891, 1990.
8. N.A.F. Jaeger and F. Rahmatian, "Integrated Optics Pockels Cell as a High Voltage Sensor," *Proceedings of the 8th Optical Fiber Sensors Conference*, pp. 153-156, Monterey, CA, Jan. 29-31, 1992.
9. F. Rahmatian and N.A.F. Jaeger, "Frequency Responses of Integrated Optics Pockels Cell High Voltage Sensors," *Proceedings of the IEEE/LEOS Annual Meeting*, pp. 462-463, Boston, MA, Nov. 16-19, 1992,.
10. "APE™ Mach-Zehnder modulator," *United technologies Photonics Technical Information*.
11. S. Thaniyavarn, "Wavelength independent, optical damage immune Z-propagating LiNbO<sub>3</sub> waveguide polarization converter," *Appl. Phys. Lett.*, vol. 47, no. 7, pp. 674-677, Oct. 1985.
12. F. Rahmatian, Integrated optics Pockels cell high-voltage sensor, M.A.Sc. thesis, Univ. of British Columbia, Vancouver, Canada, 1993.
13. A. Neyer, "Integrated-optic devices in lithium niobate: technology and applications", *SPIE*, vol. 1274, *Electro-Optic and Magneto-Optic Materials II*, pp. 2-17, 1990.
14. D. C. Erickson, "A Primer on Optical Current and Voltage Sensors and an Update on Activity," *Engineering Symposium, Bonneville Power Administration*, Mar. 31-Apr. 1, 1992.